



HAL
open science

Long-range magnetic ordering and bistability in molecular magnetism

Olivier Kahn, Yves Journaux, Corine Mathonière

► **To cite this version:**

Olivier Kahn, Yves Journaux, Corine Mathonière. Long-range magnetic ordering and bistability in molecular magnetism. Olivier Kahn. Magnetism: a supramolecular function, Kluwer Academic, pp.531-553, 1996, 0-7923-4153-8. 10.1007/978-94-015-8707-5_27. hal-04211284

HAL Id: hal-04211284

<https://hal.science/hal-04211284>

Submitted on 19 Sep 2023

HAL is a multi-disciplinary open access archive for the deposit and dissemination of scientific research documents, whether they are published or not. The documents may come from teaching and research institutions in France or abroad, or from public or private research centers.

L'archive ouverte pluridisciplinaire **HAL**, est destinée au dépôt et à la diffusion de documents scientifiques de niveau recherche, publiés ou non, émanant des établissements d'enseignement et de recherche français ou étrangers, des laboratoires publics ou privés.

LONG-RANGE MAGNETIC ORDERING AND BISTABILITY IN MOLECULAR MAGNETISM

Olivier KAHN^{a,b}, Yves JOURNAUX^a and Corine MATHONIERE^{a,b}

^a *Laboratoire de Chimie Inorganique, URA CNRS n° 420, Université de Paris Sud, 91405 Orsay, France.*

^b *Laboratoire des Sciences Moléculaires, Institut de Chimie de la Matière Condensée de Bordeaux, UPR CNRS n° 9048, 33608 Pessac, France*

1 Introduction

Molecular magnetism is a new area of research dealing with the chemistry and physics of molecular assemblies involving open-shell molecules, and polymeric structures synthesized from molecular precursors [1]. In that sense, molecular magnetism may be considered as a supramolecular function. What is important, it is to assemble the open-shell units within the lattice in such a way that the interactions between these units lead to cooperative phenomena. Cooperative here means that the lattice as a whole exhibits some physical properties which are much more than the sum of the physical properties of the units.

For more than a decade, our group has been engaged in this field. Actually, we have been more particularly concerned by two types of cooperative behaviors, namely the long-range magnetic ordering giving rise to a spontaneous magnetization below a critical temperature on the one hand, and the magnetic bistability in spin transition molecular materials on the other hand. In this short paper, we would like to illustrate our approach along both lines of research from some examples arising from the work recently performed in our research group.

2 Magnetic bricks

The first molecular-based magnets have been reported in 1986 [2,3]. Since, quite a few compounds of this kind have been described; many of them are mentioned in this book. Our specific strategy along this line consists of assembling ferrimagnetic chains or layers within the lattice in a ferromagnetic fashion [4,5]. To obtain such chains or layers, we use the brick and mortar approach. The bricks we play with are characterized by three factors, namely the shape, the chemical functionality, and the spin distribution. The first two factors are common to all facets of supramolecular chemistry. The third one is specific to molecular magnetism. Let us illustrate these ideas on an example, namely the $[\text{Cu}(\text{opba})]^{2-}$ brick shown in Figure 1, opba standing for *ortho*-phenylenebis(oxamato).

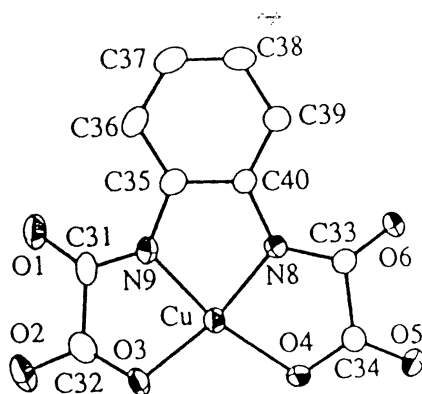


Figure 1 : Structure of $[\text{Cu}(\text{opba})]^{2-}$.

Concerning the shape, this brick is almost planar so that it is appropriate to design one- or two-dimensional networks. On the other hand, it cannot be the structuring motif of a three-dimensional network. The chemical functionality is characterized by the presence of four donating oxygen atoms, two on the left-hand and two on the right-hand side of the brick, so that $[\text{Cu}(\text{opba})]^{2-}$ can play the role of a bisbidentate ligand, and bridges two metal ions. The spin distribution factor deserves to be discussed in a more thorough manner. Experimentally, the spin distribution can be deduced from polarized neutron diffraction data [6-11]. Theoretically, it can be calculated from different methods. The most appropriate seems to be the Density Functional Theory (DFT) [12]. In the case of $[\text{Cu}(\text{opba})]^{2-}$, there is no polarized neutron diffraction data yet. The calculations indicate that the spin density arising from the Cu(II) ion (d^9 configuration) is strongly delocalized, not only toward the

oxygen and nitrogen atoms bound to the copper atom, but also toward the peripheral oxygen atoms. In addition to the positive spin densities on the copper, nitrogen, and oxygen atoms, a weak negative spin density is found on the carbon atoms of the oxamato groups, on either side of the molecular plane (π symmetry). These negative spin densities arise from spin polarization [13,14].

The spin density distribution as obtained in a DFT calculation for another Cu(II) brick, Cu(oxpn) with oxpn = N,N'-bis(3-aminopropyl)oxamido is depicted in Figure 2 [15]. Cu(oxpn) is a monobidentate ligand which can be viewed as a half of [Cu(opba)]²⁻ [16].

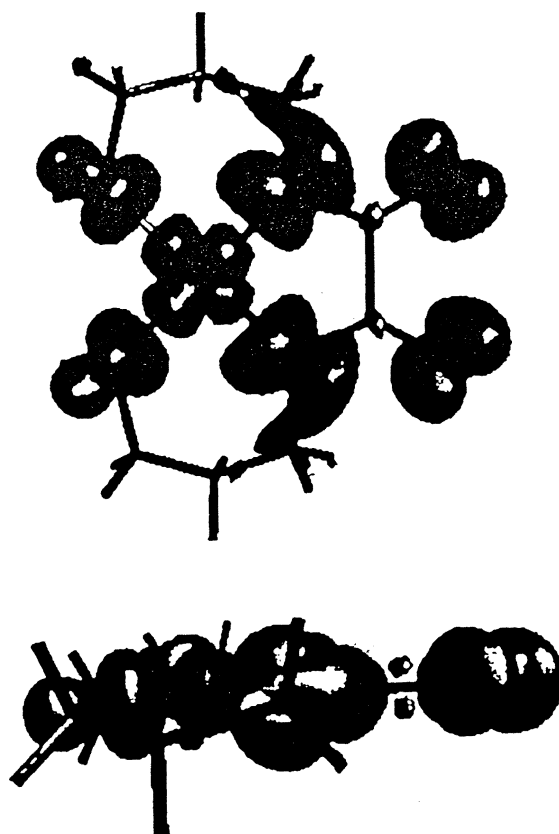


Figure 2 : Spin density distribution in Cu(oxpn) as obtained in a DFT calculation.

3 Bimetallic Ferrimagnetic Compounds

The mortar linking the bricks to each other is a magnetic metal cation, for instance Mn(II) or Co(II). The pronounced spin delocalization, due to the conjugated character of the C-N and C-O bonds, favors strong antiferromagnetic interactions between the Cu(II) ion of the brick and the Mn(II) or Co(II) ions coordinated through the oxamato oxygen atoms. Owing

to the non-compensation of the local spins, the bricks and mortar compounds display a ferrimagnetic behavior characterized by a minimum in the $\chi_M T$ versus T plot, χ_M being the molar magnetic susceptibility and T the temperature [1].

In the case of a one-dimensional ferrimagnet of formula $\text{MnCu}(\text{pba})(\text{H}_2\text{O})_3 \cdot 2\text{H}_2\text{O}$ with $\text{pba} = 1,3\text{-propylenebis(oxamato)}$, the nature of the ground state has been characterized by the spin density map in this state, deduced from both polarized neutron diffraction data and DFT calculation. The agreement between experimental and calculated maps is excellent. The results of the DFT calculation are shown in Figure 3. The map presents a large positive and almost spherical spin density around the Mn(II) ion ($S_{\text{Mn}} = 5/2$) and a weak negative spin density around the Cu(II) ion ($S_{\text{Cu}} = 1/2$) localized in the plane of the Cu(pba) fragment. It is also remarkable that despite its weakness the negative spin density arising from Cu(II) is more delocalized toward the bridging network than the positive spin density arising from Mn(II). This situation must be related to the fact that the Cu-N and Cu-O bonds are shorter and more covalent than the bridging Mn-O bonds.

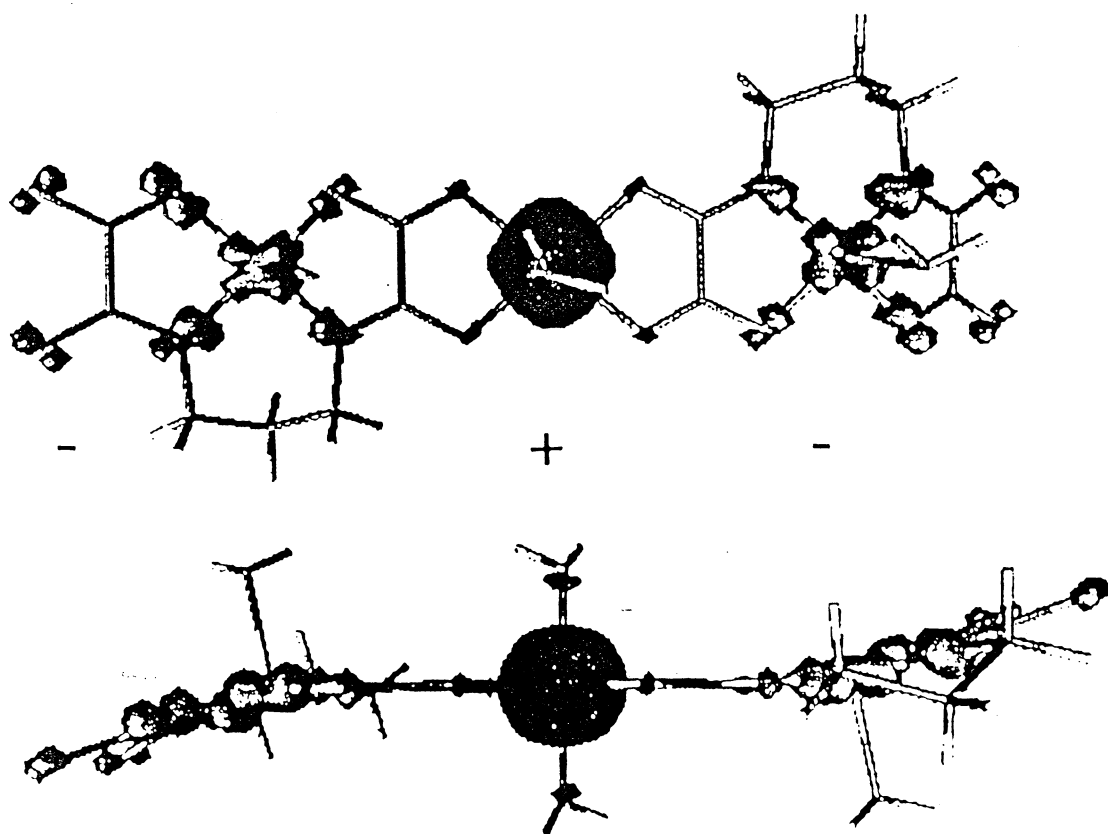


Figure 3 : Spin density map in the ground state of the one-dimensional ferrimagnet $\text{MnCu}(\text{pba})(\text{H}_2\text{O})_3 \cdot 2\text{H}_2\text{O}$

MnCu(pba)(H₂O)₃•2H₂O has a linear chain structure. On the other hand, the reaction between [Cu(opba)]²⁻ and Mn(II) in perfectly dehydrated dimethylsulfoxide (DMSO) affords a compound of formula MnCu(opba)(DMSO)₃ with a zig-zag chain structure represented in Figure 4 [18]. Two DMSO molecules are bound to the manganese atom in a *cis* position, and the third DMSO molecule occupies the apical position in the copper coordination sphere. The magnetic properties of MnCu(opba)(H₂O)₂•DMSO are typical of almost perfectly isolated ferrimagnetic chains.

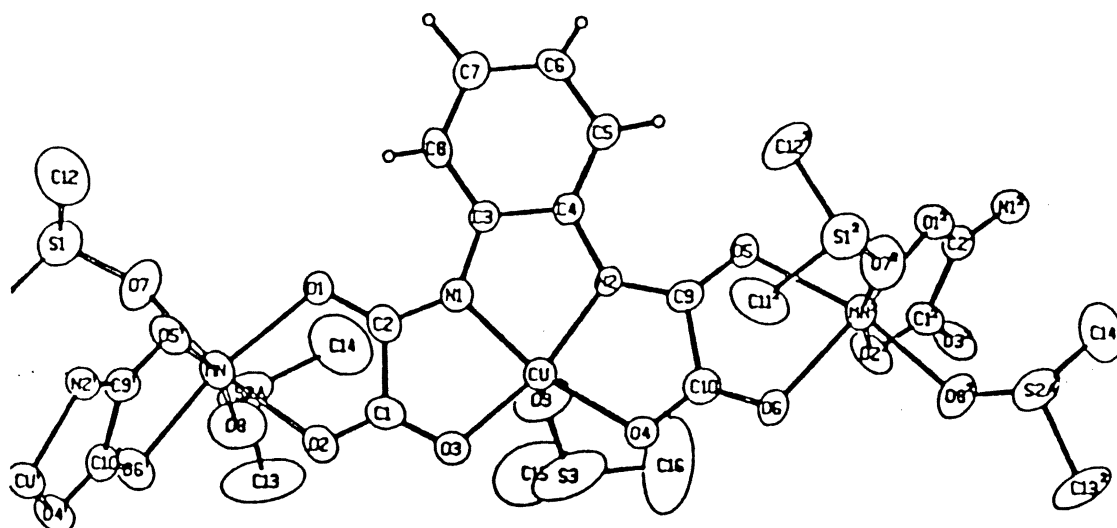


Figure 4 : Structure of the zig-zag chain compound MnCu(opba)(DMSO)₃ (from ref. 18).

4 Two-Dimensional Mn(II)Cu(II) Compounds

The zig-zag chain structure of MnCu(opba)(DMSO)₃ may suggest a strategy to increase the dimensionality of the system. This strategy consists in replacing the DMSO molecules bound to the manganese atom by the bisbidentate ligands [Cu(opba)]²⁻, which results in a crosslinking of the chains, as schematized in Figure 5. The reaction of a Mn(II) salt with (NBu₄)₂[Cu(opba)] in the 2/3 stoichiometry affords a compound of formula (NBu₄)₂Mn₂[Cu(opba)]₃•6DMSO•H₂O [17]. Up to now, it has not been possible to solve the crystal structure. However, it is most likely that this structure consists of layers with Mn₆Cu₆ edge-sharing hexagons. The manganese atom would be surrounded by three Cu(opba) groups. Such an arrangement shown in Figure 6 has actually been found in a related compound in which the tetra-

n-butylammonium cation is replaced by a radical cation [18,19]. Probably the NBu_4^+ cations and noncoordinated DMSO molecules are located between the honeycomb layers.

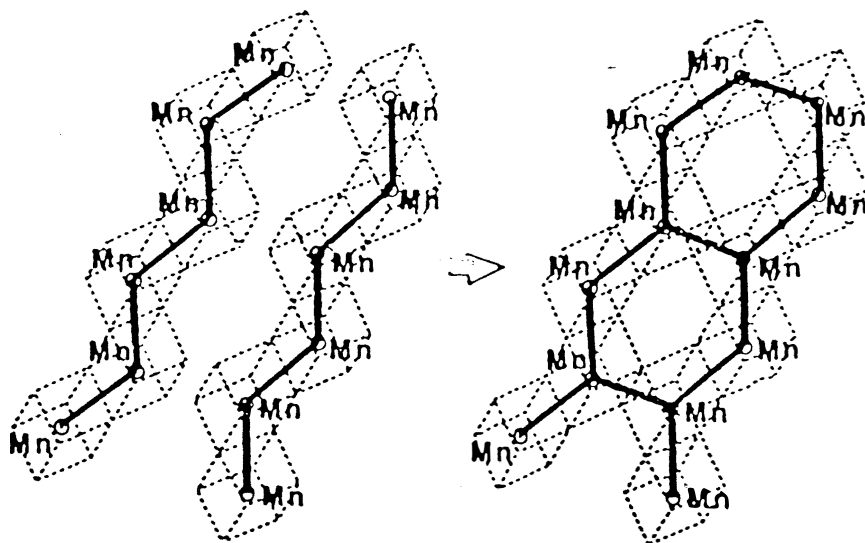


Figure 5 : Formation of a honeycomb two-dimensional lattice through crosslinking of zig-zag chains.

The magnetic behavior of $(\text{NBu}_4)_2\text{Mn}_2[\text{Cu}(\text{opba})]_3 \cdot 6\text{DMSO} \cdot \text{H}_2\text{O}$ is characteristic of a ferrimagnetic situation with Mn-Cu antiferromagnetic interactions and noncompensation of the local spins in the ground state. At $T_c = 15 \text{ K}$, a three-dimensional magnetic transition is observed with a spontaneous magnetization below this temperature. The field dependence of the magnetization at 5 K reveals a saturation magnetization of $7 \text{ N}\beta \text{ mol}^{-1}$, which confirms that in the magnetically ordered state all the $S_{\text{Mn}} = 5/2$ local spins are aligned along the field direction and the $S_{\text{Cu}} = 1/2$ local spins along the opposite direction.

The anionic copper(II) brick $[\text{Cu}(\text{opba})]^{2-}$ can be prepared with almost all kinds of counteranions, including for instance the photophysically active chromophore $[\text{Ru}(\text{bipy})_3]^{2+}$, with $\text{bipy} = 2,2'$ -bipyridine. From $[\text{Ru}(\text{bipy})_3][\text{Cu}(\text{opba})]$ we have synthesized the compound of formula $[\text{Ru}(\text{bipy})_3]\text{Mn}_2[\text{Cu}(\text{opba})]_3 \cdot 13\text{H}_2\text{O}$ in which magnetic and photophysical properties coexist [20]. As a matter of fact, this material shows a long-range magnetic ordering at $T_c = 12 \text{ K}$ along with a luminescence whose characteristics depend on the magnetic phase. We do not intend to develop here this preliminary result. However, we would like to stress that the design of molecular-based materials exhibiting two types of physical properties, if

possible in a synergistic fashion, is probably one of the main issues in this area of research [14,21].

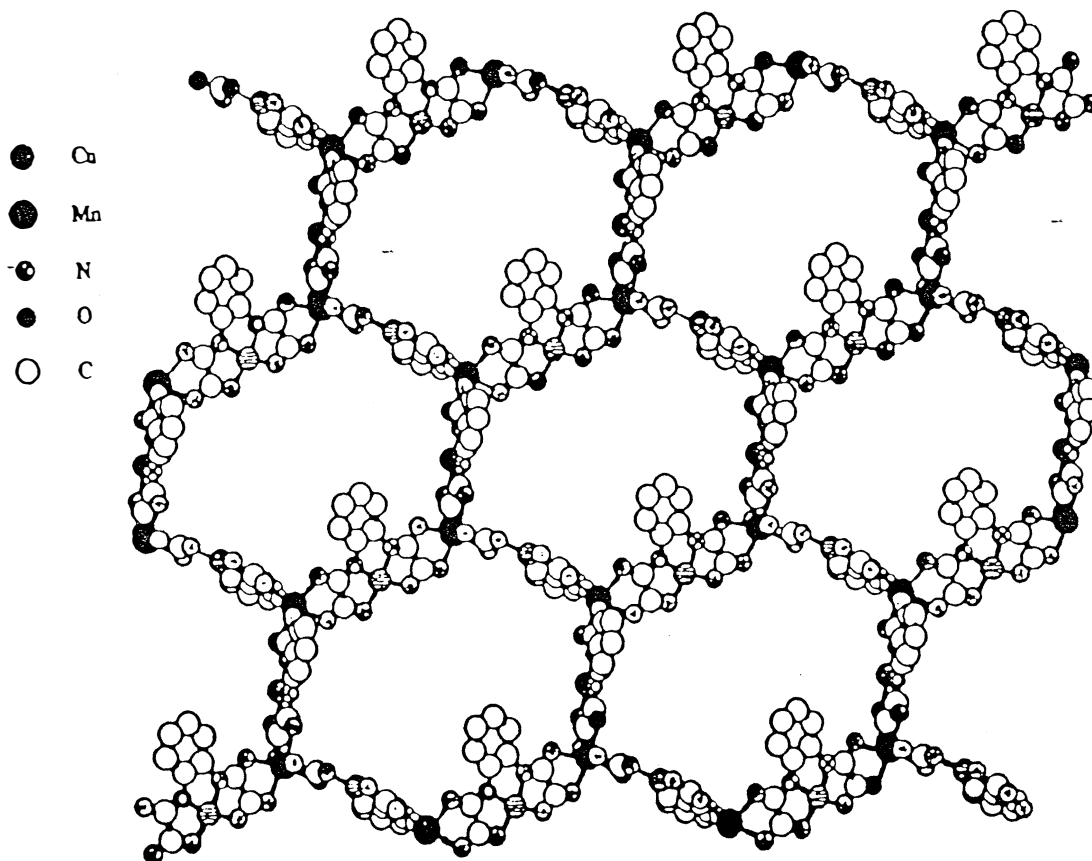
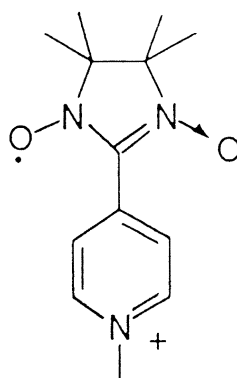


Figure 6 : Structure of a layer in $(\text{rad})_2\text{Mn}_2[\text{Cu}(\text{opba})]_3(\text{DMSO})_2 \cdot 2\text{H}_2\text{O}$, with $\text{rad}^+ = 2-(1\text{-methylpyridinium-4-yl})-4,4,5,5\text{-tetramethylimidazoline-1-oxyl-3-oxide}$ (from ref. 19).

5 A Molecular-Based Magnet with Three Kinds of Spin Carriers, and a Three-Dimensional Fully Interlocked Structure

The anionic copper(II) precursor $[\text{Cu}(\text{opba})]^{2-}$ can also be prepared with radical cations. One of them, noted rad^+ , is 2-(1-methylpyridinium-4-yl)-4,4,5,5-tetramethylimidazoline-1-oxyl-3-oxide :



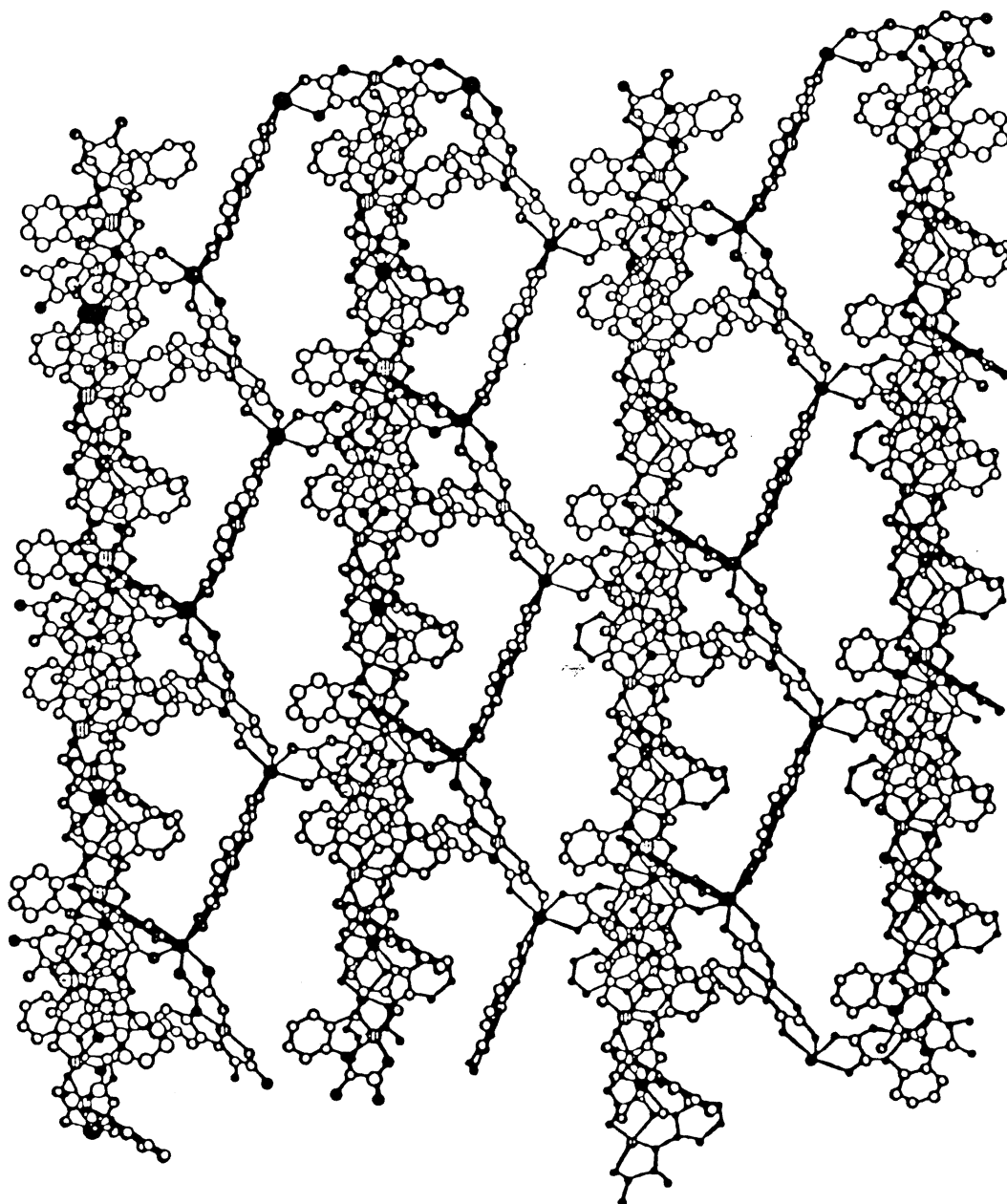


Figure 7 : Interpenetration of the two quasi perpendicular networks in $(\text{rad})_2\text{Mn}_2[\text{Cu}(\text{opba})]_3(\text{DMSO})_2 \cdot 2\text{H}_2\text{O}$ (from ref. 19).

where the unpaired electron is equally shared between the two N-O groups. The reaction of Mn(II) chloride with a large excess of $(\text{rad})_2[\text{Cu}(\text{opba})]$ in DMSO affords well-shaped single crystals of a compound of formula $(\text{rad})_2\text{Mn}_2[\text{Cu}(\text{opba})]_3(\text{DMSO})_2 \cdot 2\text{H}_2\text{O}$ [18,19]. The structure of this compound is quite amazing. There are two equivalent two-dimensional networks, noted A and B. Each network consists of honeycomb layers as shown in Figure 6. These layers stack above each other in a graphite-like fashion. The A and B networks are quasi perpendicular, and interpenetrate each other with a full interlocking of the Mn_6Cu_6 hexagons as shown in Figure 7. The topology is

that of a wire netting. The hexagons are connected further through the radical cations which bridge two copper atoms belonging to networks A and B, respectively. This affords $\text{Cu}_A\text{-rad-Cu}_B\text{-rad}$ chains. Another peculiarity of this structure concerns the chirality of the manganese sites. A manganese atom surrounded by three bidentate ligands is obviously chiral. In the structure there is a perfect alternation of Λ and Δ sites occupying the adjacent corners of a hexagon; two such sites are linked by a $\text{Cu}(\text{opba})$ group.

$(\text{rad})_2\text{Mn}_2[\text{Cu}(\text{opba})]_3(\text{DMSO})_2 \cdot 2\text{H}_2\text{O}$ exhibits a long-range magnetic ordering with the onset of a spontaneous magnetization at $T_c = 22.5$ K as shown in Figure 8. A thorough magnetic investigation reveals a peculiar behavior. The radical cations interact ferromagnetically with the $\text{Cu}(\text{II})$ ions along the $\text{Cu}_A\text{-rad-Cu}_B\text{-rad}$ chains [22]. It turns out that below T_c and in zero field the radical spins are aligned in the direction opposite to that of the $\text{Mn}(\text{II})$ spins. When the field increases, a progressive spin decoupling between the radicals and the anionic skeleton $\text{Mn}_2[\text{Cu}(\text{opba})]_3$ happens, and the radical spins tend to orient along the field direction.

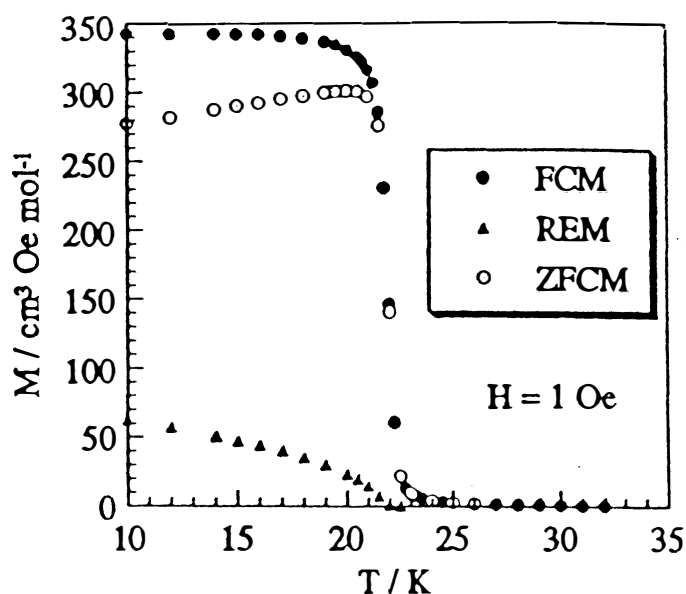


Figure 8 : Magnetization versus temperature curves for $(\text{rad})_2\text{Mn}_2[\text{Cu}(\text{opba})]_3(\text{DMSO})_2 \cdot 2\text{H}_2\text{O}$; FCM = field-cooled magnetization, REM = remnant magnetization, ZFC = zero-field-cooled magnetization (from ref. 18).

6 Co(II)Cu(II) Two-Dimensional Molecular-Based Magnets with Large Coercitive Fields

The Mn(II)Cu(II) molecular-based magnets we spoke about present a magnetic hysteresis loop with a weak coercive field, of a few tens of Oe at the most. When manganese is replaced by cobalt in a two-dimensional compound $(\text{cat})_2\text{Mn}_2[\text{Cu}(\text{opba})]_3 \cdot \text{S}$ with cat^+ standing for a cation and S for solvent molecules, a large coercive field is obtained [23]. Let us describe the magnetic properties of one of these compounds, of formula $(\text{rad})_2\text{Co}_2[\text{Cu}(\text{opba})]_3 \cdot 0.5\text{DMSO} \cdot 3\text{H}_2\text{O}$. The field-cooled-magnetization (FCM), zero-field-cooled magnetization (ZFCM), and remnant magnetization (REM) curves are displayed in Figure 9. The FCM shows a break around $T_c = 34$ K. The REM obtained in switching off the field at 2 K, and warming in zero field is strictly equal to the FCM below T_c . All the information induced by the field is retained. As for the ZFC, it is negligibly small up to 15 K. The magnetic domains are randomly oriented, and the domain walls do not move. The ZFCM slightly increases as T increases above 15 K, due to the thermal agitation which displaces the domain walls. FCM and ZFCM merge at T_c . The field dependence of the magnetization at 1.7 K shown in Figure 10 reveals a hysteresis loop with a coercive field as large as 3.0 kOe and a remnant magnetization of about $7 \times 10^3 \text{ cm}^3 \text{ Oe mol}^{-1}$.

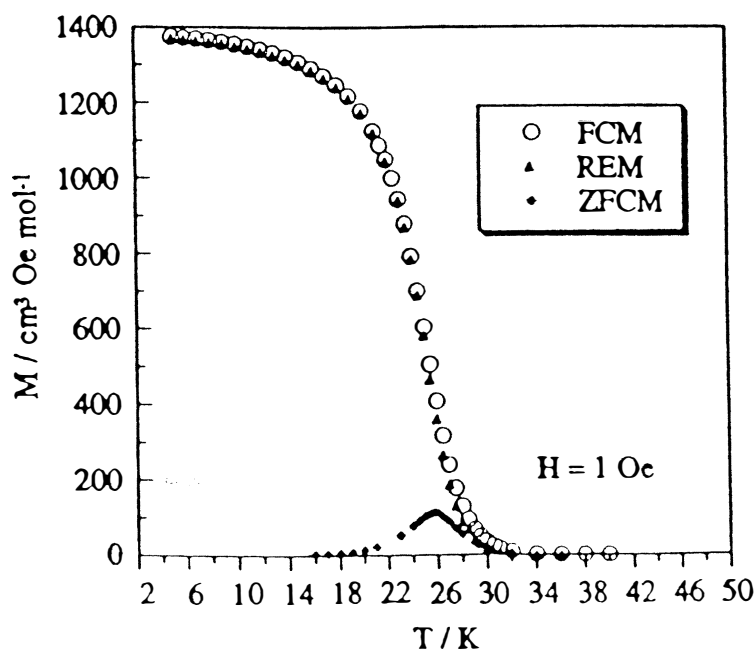


Figure 9 : Magnetization versus temperature curves for $(\text{rad})_2\text{Co}_2[\text{Cu}(\text{opba})]_3 \cdot 0.5\text{DMSO} \cdot 3\text{H}_2\text{O}$ (from ref. 23).

The strong coercivity observed in these Co(II)Cu(II) compounds is most probably due to the unquenched orbital momentum of the Co(II) ion in octahedral surroundings.

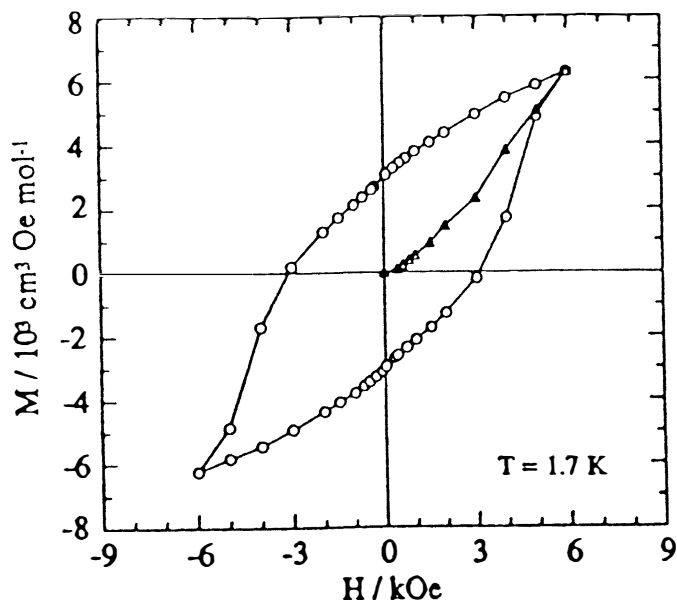


Figure 10 : Magnetic hysteresis loop at 1.7 K for $(\text{rad})_2\text{Co}_2[\text{Cu}(\text{opba})]_3 \cdot 0.5\text{DMSO} \cdot 3\text{H}_2\text{O}$ (from ref. 23).

7 Spin Transition Molecular Materials

In some transition metal compounds, in particular in those containing $3d^4$ - $3d^7$ metal ions in octahedral surroundings, a crossover between a low-spin (LS) and a high-spin (HS) state may happen. Such a spin crossover may be induced by a variation of temperature, of pressure or by a light-irradiation [24-31]. This phenomenon probably represents the most spectacular example of molecular bistability [32,33]. Our main objective in the field of spin-crossover compounds is to design and synthesize compounds exhibiting a large thermal hysteresis, and to explore to what extent these compounds could be used as active elements in memory devices. Our first step along this line deals with a display device. For that, some requirements must be fulfilled, which can be summed up as follows : (i) the transition must be abrupt both in the warming mode at $T_C \uparrow$ and in the cooling mode at $T_C \downarrow$; (ii) it must occur with a large thermal hysteresis effect. The bistability is achieved in the temperature range between $T_C \uparrow$ and $T_C \downarrow$; (iii) for an all-public application, the transition temperatures must be as close as possible to room temperature. The ideal situation is that where the ambient temperature falls in the middle of the thermal hysteresis loop; (iv) the transition between LS and HS states must be

accompanied by an easily detectable response, such as a change of color [34]. The first two requirements are related to the cooperativity, i.e. to the magnitude of the interactions between active sites. In purely molecular crystals containing spin-crossover mononuclear entities, the intermolecular interactions are very weak, of the van der Waals type. Such mononuclear compounds seem not to be appropriate for our purpose. In many cases, the spin-transition mononuclear entities are hydrogen bonded within the crystal lattice. These hydrogen bonds may lead to stronger intermolecular interactions. This situation is most often achieved when the crystal lattice contains some non-coordinated solvent molecules. Even larger interactions between active sites may be anticipated if these active sites are covalently linked by chemical bridges, in particular if these bridges are conjugated. Our starting idea, illustrated in Figure 11, is that in polymeric spin-transition compounds the cooperativity should be magnified.

The first experimental result supporting this idea was provided by the compound $[\text{Fe}(\text{btrz})_2(\text{NCS})_2] \cdot \text{H}_2\text{O}$ with btrz = bis-1,2,4-triazole whose structure is depicted in Figure 12 [35]. Each iron atom is surrounded by two NCS groups in trans position and four btrz ligands coordinated through the nitrogen 1- and 1'-positions. The btrz ligands bridge the iron atoms, which results in a two-dimensional structure. The non-coordinated water molecules are hydrogen bonded to the nitrogen atoms of btrz occupying the 2- and 2'-positions. This two-dimensional compound shows extremely abrupt spin transitions at $T_c \uparrow = 144.5 \text{ K}$ and $T_c \downarrow = 123.5 \text{ K}$ (see Figure 12). The thermal hysteresis width is of 21 K. Between $T_c \uparrow$ and $T_c \downarrow$ the state of the system depends on its history.

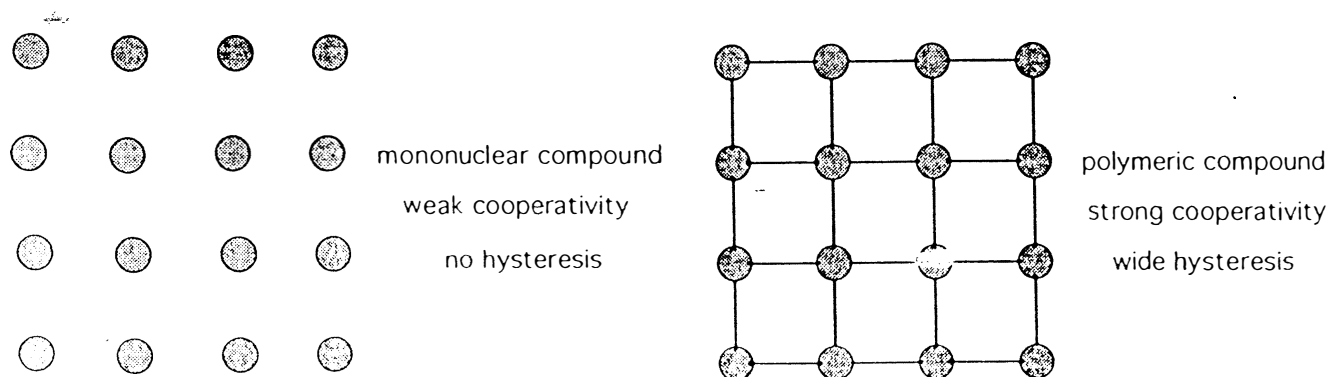


Figure 11 : Cooperativity in spin-transition mononuclear and polymeric species.

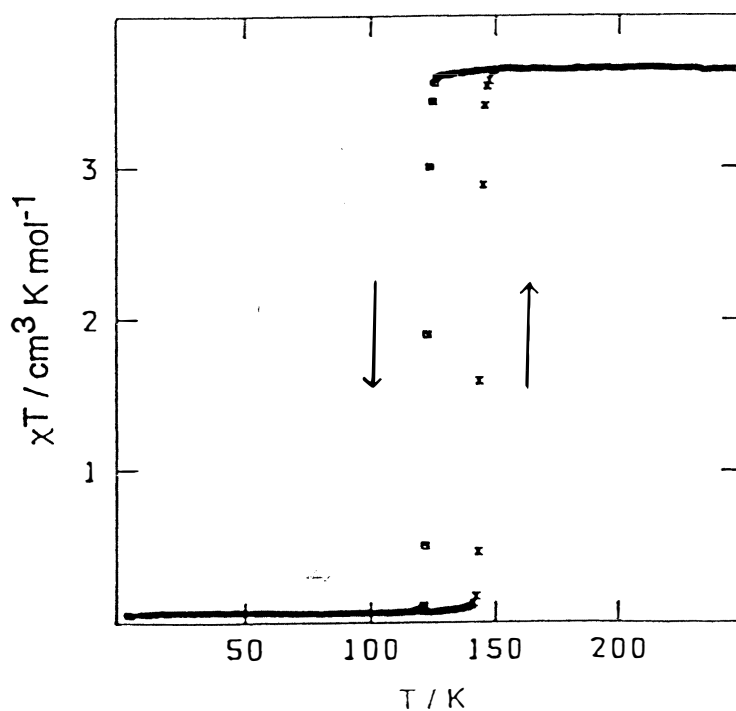
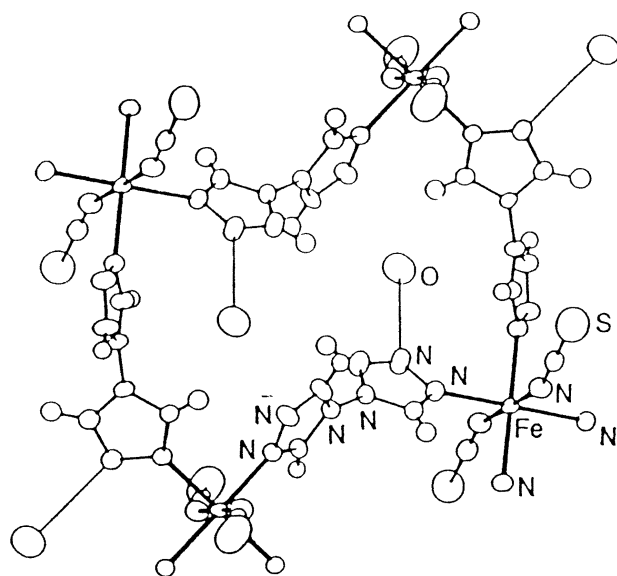


Figure 12 : Structure of $[\text{Fe}(\text{btrz})_2(\text{NCS})_2] \cdot \text{H}_2\text{O}$ and $\chi_{\text{M}}T$ versus T curves in the warming and cooling modes for this compound (from ref. 35).

8 Thermal Hysteresis Loop for $[\text{Fe}(\text{Htrz})_2(\text{trz})](\text{BF}_4)$

It is in 1977 that for the first time a Fe(II) - triazole compound showing a spin transition above room temperature accompanied with a purple - white change of color was mentioned [36]. Later on, a russian group reported on a series of iron(II) - 1,2,4-triazole compounds, several of them exhibiting spin transitions around room temperature with thermal hysteresis and thermochromic effects

[37,38]. More recently Goodwin and coworkers also investigated these compounds [39]. A few years ago, it occurred to us that the compounds of this family could fulfill the criteria mentioned above, and we decided to investigate them in a thorough manner.

The reaction of $[\text{Fe}(\text{H}_2\text{O})_6](\text{BF}_4)_2$ on 1,2,4-*H*-triazole affords two compounds depending on the experimental conditions. The former compound is $[\text{Fe}(\text{Htrz})_2(\text{trz})](\text{BF}_4)$; a spontaneous deprotonation of one out of three Htrz ligands occurs. The latter compound is $[\text{Fe}(\text{Htrz})_3](\text{BF}_4)_2 \cdot \text{H}_2\text{O}$; no deprotonation occurs, and the three ligands are neutral. We will restrict here to one the modifications of the former compound, obtained by adding a solution of 1,2,4-*H*-trz dissolved in ethanol to a solution of the iron(II) salt dissolved in water [40].

A large variety of physical techniques have been utilized to characterize the spin transition regime of this compound. Both in the warming and cooling modes the spin transition is exceptionally abrupt. It is also accompanied with a well pronounced thermochromism between the purple color in the LS state and the white color in the HS state. The purple color in the LS state arises from the ${}^1\text{A}_{1g} \rightarrow {}^1\text{T}_{1g}$ d - d absorption at 520 nm. In the HS, the spin-allowed absorption of lowest energy appears at 800 nm, at the limit of the infra-red range. The transition temperatures are found to be very slightly dependent on both the sample and of the technique used to detect the transition. They may be given as $T_c \uparrow = 383 \pm 3$ K and $T_c \downarrow = 345 \pm 2$ K. The thermal hysteresis width is then about 40 K.

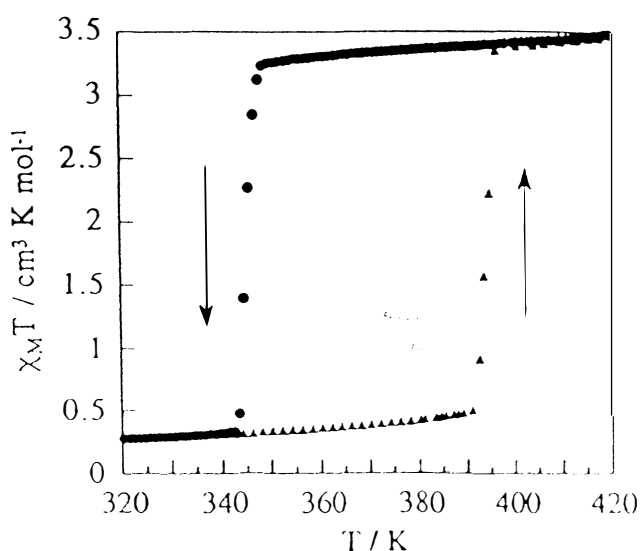


Figure 13 : $\chi_M T$ versus T curve in the warming and cooling modes for $[\text{Fe}(\text{Htrz})_2(\text{trz})](\text{BF}_4)$ (from ref. 40).

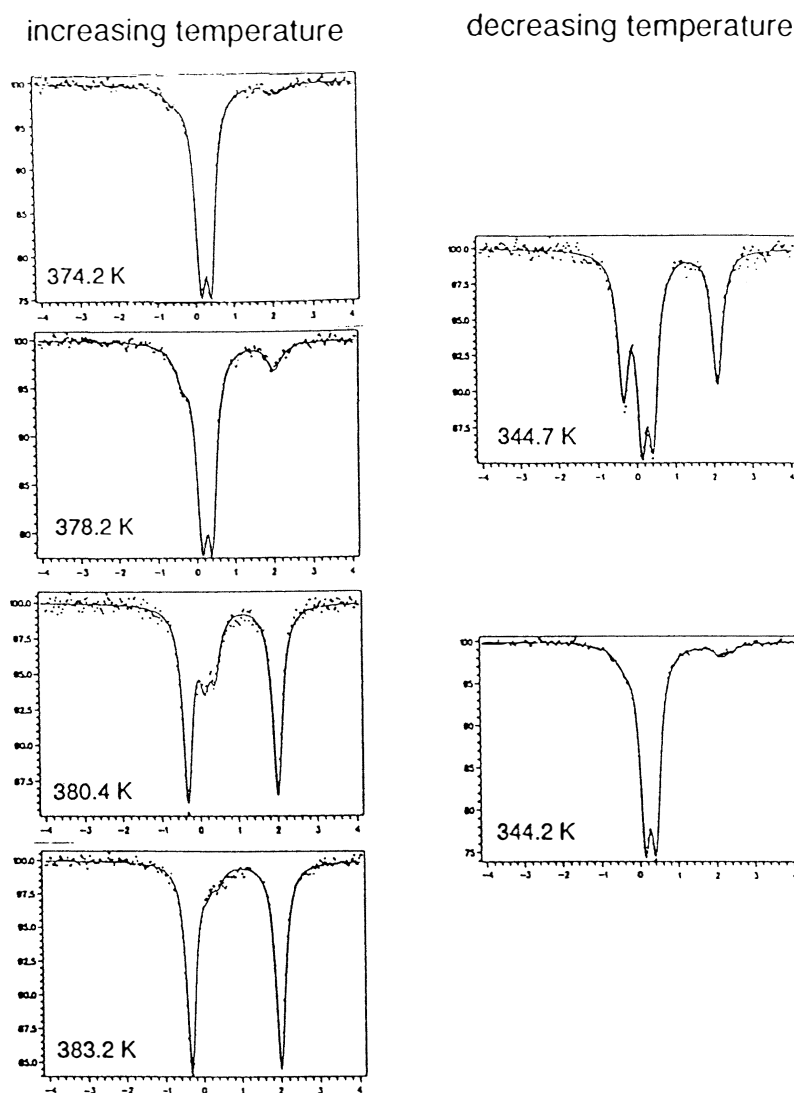


Figure 14 : Mössbauer spectra at various temperatures for $[\text{Fe}(\text{Htrz})_2(\text{trz})](\text{BF}_4)$ (from ref. 40).

Let us briefly comment on the physical data. The magnetic properties are shown in Figure 13 in the form of the $\chi_M T$ versus T plot. Above $T_c \uparrow$ in the warming mode and $T_c \downarrow$ in the cooling mode $\chi_M T$ is equal to $3.4(1) \text{ cm}^3 \text{ K mol}^{-1}$, which corresponds to what is expected for an octahedral iron(II) compound in the HS state. Below the transition temperatures $\chi_M T$ is equal to about $0.3 \text{ cm}^3 \text{ K mol}^{-1}$, which indicates that there is a small residual fraction of HS molecules in the LS phase.

The Mössbauer spectroscopy confirms the magnetic data. Typical spectra are represented in Figure 14. The spectrum is characteristic of a HS iron(II) compound above 400 K, and of a LS iron(II) compound below 340 K. The two spectra coexist within a few Kelvin both in the warming and cooling modes. The spectra do not show any dynamical broadening of the

Mössbauer lines, thus indicating that the conversion rates remain lower than the Mössbauer hyperfine frequency (around 10^7 s^{-1}), despite the fact that the transitions take place above room temperature. The slowing down of the conversion rates as compared to other iron(II) spin transition compounds might be due to the polymeric nature of the compound.

The differential scanning calorimetry (DSC) curves are represented in Figure 15. They show an abrupt endothermic process at $T_c \uparrow$ in the warming mode, and an even more abrupt exothermic process at $T_c \downarrow$ in the cooling mode. The enthalpy variations associated with these processes are found equal to 27.8 and 28.6 kJ mol^{-1} , respectively. These values are much higher than those found for the mononuclear iron(II) spin-transition compounds, usually in the 5 - 15 kJ mol^{-1} range. For instance, the enthalpy variation for $\text{Fe}(\text{phen})_2(\text{NCS})_2$ with phen = *ortho*-phenanthroline is equal to 8.59 kJ mol^{-1} .

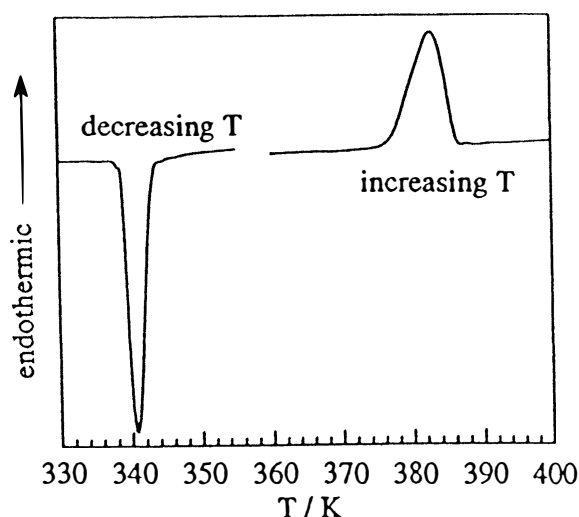


Figure 15 : Differential scanning calorimetry curves $[\text{Fe}(\text{Htrz})_2(\text{trz})](\text{BF}_4)$ (from ref. 40)

As already pointed out, the spin transition in all the Fe(II) - 1,2,4-trz compounds is accompanied by a dramatic change of color, so that the transitions can be detected optically, using the set up schematized in Figure 16. This set up records changes in optical properties of spin transition compounds in a remarkably simple and reliable way. The sample holder containing about 50 mg of microcrystalline compound is fitted to the common end of a double optical fiber, and plugged into a cryogenic system. The temperature rises and decreases at the rate of 1 Kelvin per minute without overshooting. A photomultiplier provided with a 520 nm interferential filter converts the light reflected by the sample into an electric current whose intensity depends on the color change. As the spin transition compound absorbs at 520 nm in the LS

state and not in the HS state, the intensity recorded is null for the purple color (LS state), and maximum for the white color (HS state). A personal computer is used to control the process and record the data. One can then convert the arbitrary intensities into normalized HS molar fractions, identical to what is obtained with other techniques.

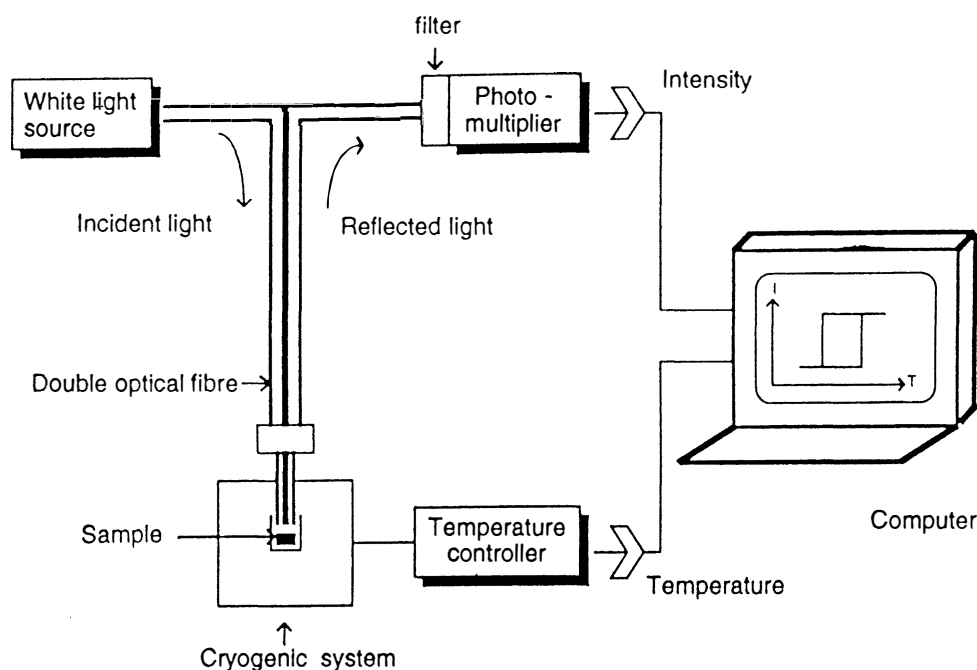


Figure 16 : Device used for the optical detection of the spin transition in the Fe(II) - 1,2,4-triazole compounds.

In spite of many efforts it has not been possible yet to grow single crystals of $[\text{Fe}(\text{Htrz})_2(\text{trz})](\text{BF}_4)$, and structural information has been obtained from alternative techniques such as EXAFS at the iron edge and X-ray powder diffraction [41].

The EXAFS data led to a rather accurate description of the basic structure. This structure consists of linear chains in which the Fe(II) ions are triply bridged by triazole ligands through the nitrogen atoms occupying the 1- and 2-positions, as represented in Figure 17. One out of three triazole rings is deprotonated, and probably a proton hole in $[\text{Fe}(\text{Htrz})_2(\text{trz})](\text{BF}_4)$ is disordered over each $\text{Fe}(\text{Htrz})_2(\text{trz})\text{Fe}$ bridging network, so that the three-fold symmetry of the chain compound depicted in Figure 17 is retained.

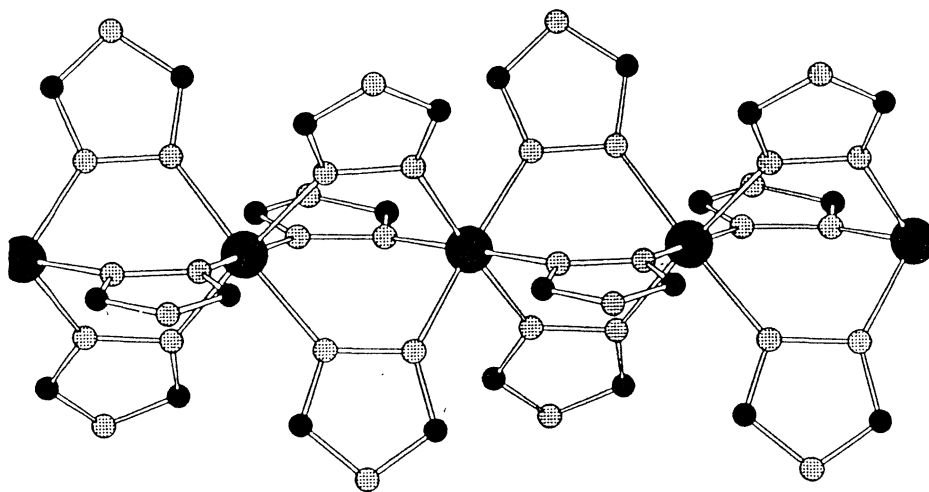


Figure 17 : Structure of the polymeric Fe(II) - 1,2,4-triazole compounds, as deduced from the EXAFS investigation (from ref. 41).

9 Molecular Alloys

We have seen that one of our main targets was to synthesize spin-transition compounds for which room temperature exactly falls in the middle of the thermal hysteresis loop. Using the trial and error method, such compounds can be obtained. We synthesized, for instance, $[\text{Fe}(\text{NH}_2\text{trz})_2]\text{Br}_2 \cdot \text{H}_2\text{O}$ which shows a spin transition regime with $T_c^\uparrow = 307 \text{ K}$ and $T_c^\downarrow = 279 \text{ K}$. The center of the hysteresis loop is 293 K , i.e. exactly at room temperature. However, the transition in the cooling mode is rather gradual, so that this compound cannot be used in a display device [34]. We are presently exploring the iron(II) - triazole system as a whole. We will not enter into the details of our findings here. Rather, we would like to focus on another approach to obtain the ideal compound. This approach is based on the concept of spin-transition molecular alloys.

Let us explicit what we mean by "molecular alloy". We know that the compounds with the stoichiometry $[\text{Fe}(\text{R}_1\text{trz})_3]\text{A}_2$ or $[\text{Fe}(\text{R}_2\text{trz})_2(\text{trz})]\text{A}$ where A is a monovalent anion have a one-dimensional polymeric structure. Let us assume now that we can synthesize two compounds of this sort, of formula $[\text{Fe}(\text{R}_1\text{trz})_3]\text{A}_2$ and $[\text{Fe}(\text{R}_2\text{trz})_3]\text{A}_2$, respectively, R_1trz and R_2trz being two different 4-substituted-1,2,4-triazole ligands. We assume further that both compounds exhibit a spin transition, the former around the temperature T_1 and the latter around T_2 . T_1 and T_2 may be defined as the middles of the thermal

hysteresis loops. If we mix 50% of $[\text{Fe}(\text{R}_1\text{trz})_3]\text{A}_2$ and $[\text{Fe}(\text{R}_2\text{trz})_3]\text{A}_2$ in the solid state, we obviously end up with a material containing 50% of chains $[\text{Fe}(\text{R}_1\text{trz})_3]_\infty$ and 50% of chains $[\text{Fe}(\text{R}_2\text{trz})_3]_\infty$. This material will display a two-step spin transition regime, one step occurring around T_1 and the other step occurring around T_2 . On the other hand, if we react the $[\text{Fe}(\text{H}_2\text{O})_6]\text{A}_2$ salt with a mixture of 50% of R_1trz and 50% of R_2trz dissolved in a common solvent, we end up with another material in which now all the chains have a mixed composition with 50% of each of the two ligands, as emphasized in Figure 18. Such a material is defined as a molecular alloy, and owing to the interactions between the $\text{Fe}(\text{II})$ ions along the chain, a mean effect may be expected. In such a case, rather abrupt transitions around $T = (T_1 + T_2)/2$ might be observed. In other words, the molecular alloy of formula $[\text{Fe}(\text{R}_1\text{trz})_{1.5}(\text{R}_2\text{trz})_{1.5}]\text{A}_2$ could exhibit a spin transition regime that no pure compound exhibits. More generally, the spin transition regime of the molecular alloys $[\text{Fe}(\text{R}_1\text{trz})_{3-x}(\text{R}_2\text{trz})_{3x}]\text{A}_2$ might be fine-tuned through the x value specifying the chemical composition of the alloy.

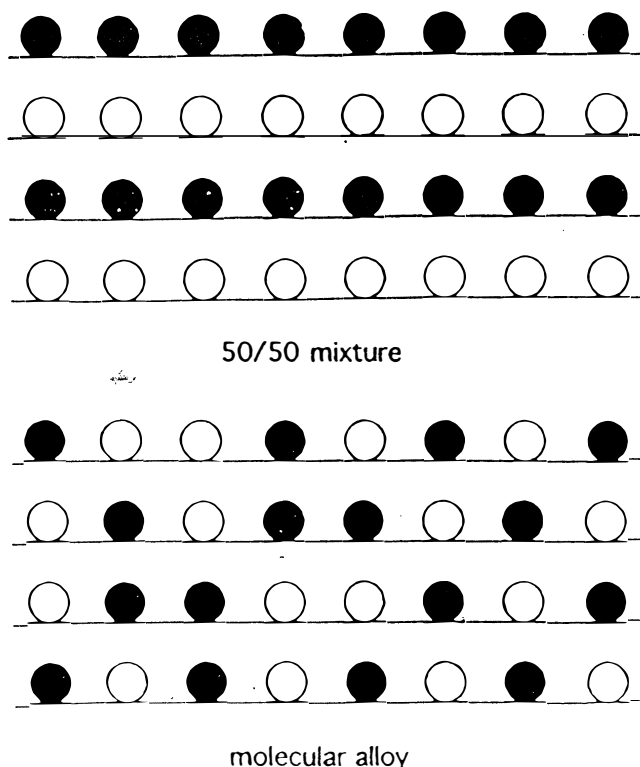


Figure 18 : Schematic representation of the structural difference between a 50/50 mixture and a molecular alloy with the same composition. The white and dark balls symbolize the R_1trz and R_2trz ligands, respectively.

We are engaged in a thorough investigation of this completely new phenomenon. Here, we restrict ourselves to one example, concerning the system $[\text{Fe}(\text{Htrz})_{3-3x}(\text{NH}_2\text{trz})_{3x}](\text{ClO}_4)_2 \cdot n\text{H}_2\text{O}$. Both T_c^\uparrow and T_c^\downarrow decrease almost linearly with x . For $x = 0$, T_c^\uparrow and T_c^\downarrow are equal to 321 K and 296 K, respectively. For small x values, when x increases of 0.01, T_c^\uparrow decreases of 1.8 K and T_c^\downarrow of 1.6 K. For $x = 0.05$, the transition occurs on either side of room temperature, with $T_c^\uparrow = 304$ K and $T_c^\downarrow = 288$ K, as shown in Figure 19. At 295 K, one may observe a purple compound in its $S = 0$ state or a white compound in a $S = 2$ state, depending on the history of the sample [42]. Both states are stable at room temperature. A gentle cooling (for instance by dipping the tube containing the alloy in acetone and evaporating acetone) or a gentle warming of the sample is sufficient to induce the transition.

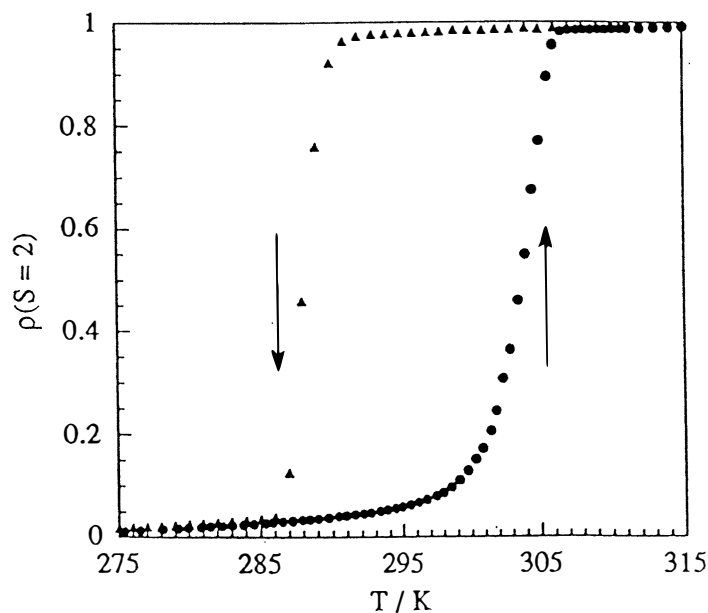


Figure 19 : Thermal hysteresis loop at room temperature for $[\text{Fe}(\text{Htrz})_{2.85}(\text{NH}_2\text{trz})_{0.15}](\text{ClO}_4)_2 \cdot \text{H}_2\text{O}$.

10 Concluding Remarks

In this paper, we only presented a small part of our work in the field of molecular magnetism. One of the main specificity of this field is its interdisciplinary character. It meets together organic, organometallic and inorganic chemists as well as theoreticians, physicists, life science and material science people. The heart of our activity deals with the synthesis of novel chemical objects involving open-shell units. To understand the properties of these objects, we need to use the basic concepts of physics. Sometime, some of

these objects may be utilized in genuine memory devices. It is for instance the case for our spin transition materials showing a magnetic bistability around room temperature. As a conclusion, we would like to point out that this area of research combines the beauty, the aesthetic appeal of supramolecular chemistry and the excitement of a new physics.

References

1. Kahn, O. (1993) *Molecular Magnetism*, VCH, New York.
2. Miller, J. S., Calabrese, J. C., Epstein, A. J., Bigelow, R. W., Zang, J. H., Reiff, W. M. (1986) *J. Chem. Soc., Chem. Commun.* 1026.
3. Pei, Y., Verdaguer, M., Kahn, O., Sletten, J., Renard, J. P. (1986) *J. Am. Chem. Soc.* **108**, 428.
4. Kahn, O. (1987) *Struct. Bonding (Berlin)* **68**, 89.
5. Kahn, O. (1995) *Adv. Inorg. Chem.* **43**, 179.
6. Brown, P. J., Capiomont, A., Gillon, B., and Schweizer, J. (1979) *J. Mag. Mag. Mat.* **14**, 289.
7. Figgis, B. N., Mason, R., Smith, A. R. P., Vargese, J. N., and William, G. A. (1983) *J. Chem. Soc. Dalton Trans.* 703.
8. Zheludev, A., Barone, V., Bonnet, M., Delley, B., Grand, A., Ressouche, E., Rey, P., Subra, R. and Schweizer, J. (1994) *J. Am. Chem. Soc.* **116**, 2019.
9. Zheludev, A., Grand, A., Ressouche, E., Schweizer, J., Morin, B. G., Epstein, A. J., Dixon, D. A., and Miller, J. S. (1994) *J. Am. Chem. Soc.* **116**, 7243.
10. Ressouche, E., Boucherle, J. X., Gillon, B., Rey, P., and Schweizer, J. (1993) *J. Am. Chem. Soc.* **115**, 3610.
11. Gillon, B., Cavata, C., Schweiss, P., Journaux, Y., Kahn, O., and Schneider, D. (1989) *J. Am. Chem. Soc.* **111**, 7124.
12. Becke, A. D. (1989) *Density Functional Theories in Quantum Chemistry: Beyond the Local Density Approximation*, Becke, A. D. Ed., A.C.S. Symposium Series, Washington D.C., vol. 394, pp. 166 and references therein.
13. Kollmar, C., and Kahn, O. (1993) *Acc. Chem. Res.* **26**, 259.
14. Kahn, O. (1994) *Comments Cond. Mat. Phys.* **17**, 39.
15. Baron, V., Gillon, B., Gousson, A., Mathonière, C., Kahn, O., Grand, A., Ölstromd, L., Tellgren, R., Delley, B. manuscript in preparation.
16. Mathonière, C., and Kahn, O. (1994) *Inorg. Chem.* **33**, 2103.
17. Stumpf, H. O., Pei, Y., Kahn, O., Sletten, J., and Renard, J.P. (1993) *J. Am. Chem. Soc.* **115**, 6738.
18. Stumpf, H. O., Ouahab, L., Pei, Y., Grandjean, D., and Kahn, O. (1993) *Science* **261**, 447.
19. Stumpf, H. O., Ouahab, L., Pei, Y., Bergerat, P., and Kahn, O. (1994) *J. Am. Chem. Soc.* **116**, 3866.
20. Turner, S. S., Michaut, C., Kahn, O., Ouahab, L., Lecas, A., and Amouyal, E. (1995) *New. J. Chem.* **19**, 773.
21. Day, P. (1993) *Science* **261**, 431.

22. Caneschi, A., Gatteschi, D., Sessoli, R., and Rey, P. (1989) *Acc. Chem. Res.* **22**, 392.
23. Stumpf, H. O., Pei, Y., Michaut, C., Kahn, O., Renard, J. P., and Ouahab, L. (1994) *Chem. Mater.* **6**, 257.
24. Goodwin, H. A. (1976) *Coord. Chem. Rev.* **18**, 293.
25. Gütlich, P. (1981) *Struct. Bonding (Berlin)* **44**, 83.
26. Gütlich, P., Hauser, A. (1990) *Coord. Chem. Rev.* **97**, 1.
27. Gütlich, P., Hauser, A., Spiering, H. (1994) *Angew. Chem. Int. Ed. Engl.* **33**, 2024.
28. König, E., Ritter, G., Kulshreshtha, S. K. (1985) *Chem. Rev.* **85**, 219.
29. König, E. (1987) *Prog. Inorg. Chem.* **35**, 527.
30. König, E. (1991) *Struct. Bonding (Berlin)* **76**, 51.
31. Roux, C., Zarembowitch, J., Gallois, B., Granier, T., Claude, R. (1994) *Inorg. Chem.* **33**, 2273.
32. Kahn, O., Launay, J. P. (1988) *Chemtronics* **3**, 140.
33. Zarembowitch, J., Kahn, O. (1991) *New J. Chem.* **15**, 181.
34. Kahn, O., Kröber, J., Jay, C. (1992) *Adv. Mater.* **4**, 718.
35. Vreugdenhil, W., van Diemen, J. H., de Graaff, R. A. G., Haasnoot, J. G., Reedijk, J., van der Kraan, A. M., Kahn, O., Zarembowitch, J. (1990) *Polyhedron* **9**, 2971.
36. Haasnoot, J. G., Vos, G., Groeneveld, W. L. (1977) *Z. Naturforsch. B* **32**, 421.
37. Lavrenova, L. G., Ikorskii, V. N., Varnek, V. A., Oglezneva, I. M., Larionov S. V. (1986) *Koord. Khim.* **12**, 207.
38. Lavrenova, L. G., Ikorskii, V. N., Varnek, V. A., Oglezneva, I. M., Larionov S. V. (1991) *Koord. Khim.* **16**, 654.
39. Sugiyarto, K. H., Goodwin, H. A. (1994) *Aust. J. Chem.* **47**, 263.
40. Kröber, J., Audière, J. P., Claude, R., Codjovi, E., Kahn, O., Haasnoot, J. G., Grolrière, F., Jay C., Bousseksou, A., Linares, J., Varret, F., Gonthier-Vassal, A. (1994) *Chem. Mater.* **6**, 1404.
41. Michalowicz, A., Moscovici, J., Ducourant, B., Cracco, D., Kahn, O. (1995) *Chem. Mater.* **7**, 1833.
42. Kröber, J., Codjovi, E., Kahn, O., Groslière, F., Jay, F. (1993) *J. Am. Chem. Soc.* **115**, 9810.